Reviews
doi.org/10.1002/celc.202100093

Chemistry Europe
European Chemical Societies Publishing

Methods for the Determination of Valid Impedance Spectra in Non-stationary Electrochemical Systems: Concepts and Techniques of Practical Importance

Krisztina J. Szekeres, Soma Vesztergom, Maria Ujvári, and Győző G. Láng*[a]

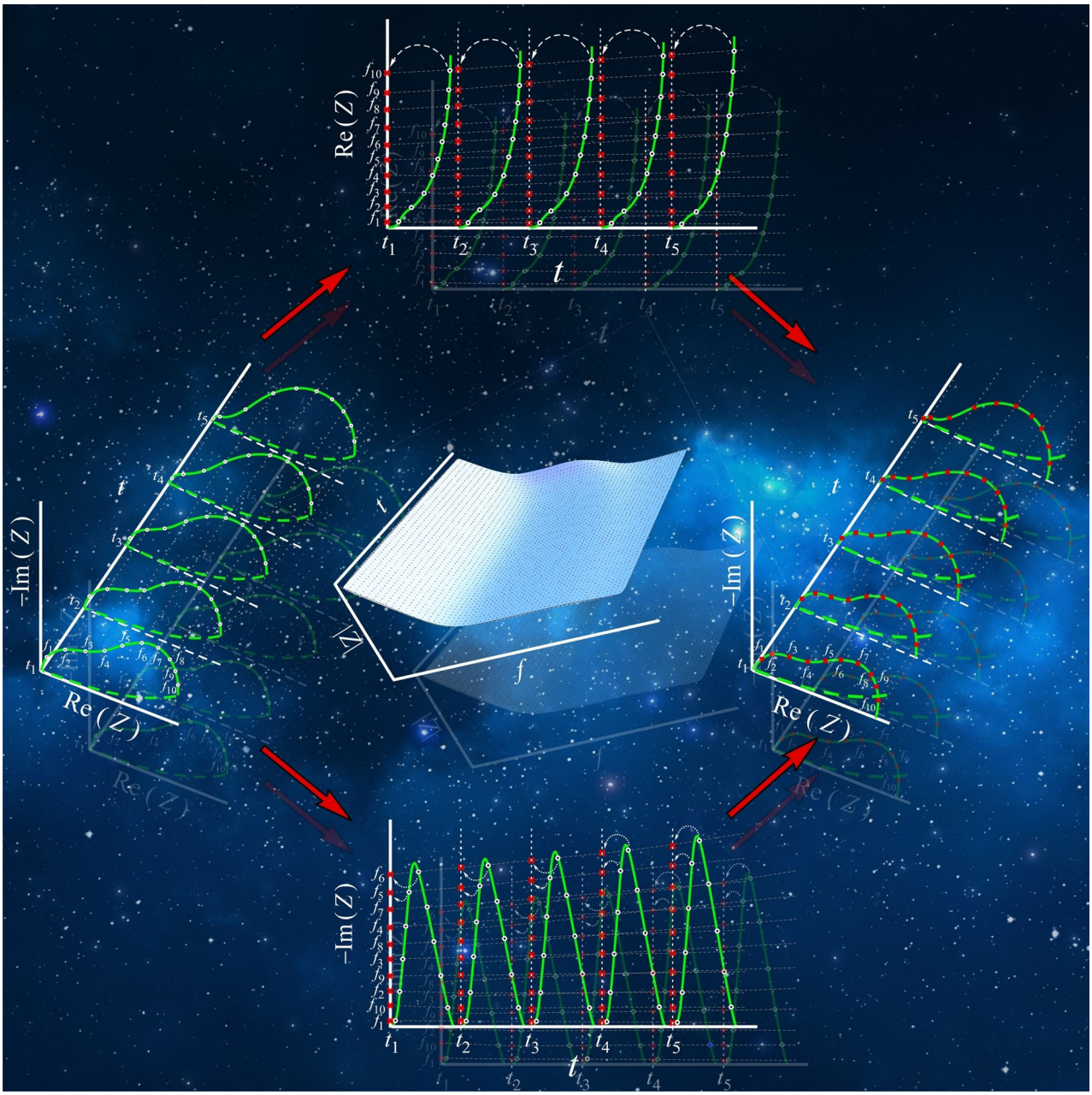

Electrochemical impedance spectroscopy (EIS) is a widely used technique for characterizing electrochemical systems. The term "electrochemical impedance spectroscopy" actually has a two-fold meaning: it is both a measurement technique to determine impedance spectra and an analysis tool for extracting information about an electrochemical system. Contrary to some opinions, the design of valid EIS measurements is not trivial in practice, as systems under test also have to meet certain requirements to ensure the validity of the measured data. One of the most serious and underestimated problems is that many electrochemical systems (including biological, reacting, and corroding systems) are intrinsically non-stationary and are affected by time-dependent phenomena. This study provides an overview and guidance on some of the methodologies proposed in the literature to address problems related to impedance measurements in time-varying (non-stationary) systems. Selected techniques for the determination of "true" impedance spectra in non-stationary systems are briefly reviewed. To better understand the theoretical background of the different approaches, basic principles of the measuring methods and the fundamentals of data collection, validation, and correction are also discussed.

1. Introduction

Electrochemical impedance spectroscopy (EIS) is a widely used, powerful tool for investigation of charge transfer and charge transport processes occurring in electrochemical systems.[1–8] The term "spectroscopy" in the name of the method is justified, since any study of how absorption of electromagnetic radiation depends on frequency can be considered as spectroscopy. A plot containing the intensity of the absorption, i.e., the electrochemical impedance, with respect to the frequency is called a "spectrum".

The essence of the method is the application of an electrical stimulus or perturbation (voltage or current) to the system under test and to observe the (current or potential) response. The perturbation can be applied in many forms, e.g., as a step function (i.), a noise signal (ii.) a sinusoidal signal (iii.) or a multisine signal (iv.), etc. In case (i.) a step signal is applied at a time t_0, and the time-dependent response $y(t–t_0)$ is measured. In case (ii.) a continuous voltage signal composed of random noise with energy over a predetermined frequency range is applied to the system, and the time dependent current response is measured. Fourier transform (see Appendix A) provides the link between the time- and frequency domain in both cases.[9–14] In case (iii.) a single-frequency sinusoidal AC voltage or current signal is applied to the system and the resulting current or voltage is measured. The classical "frequency by frequency" mode of impedance measurements (the "single sine excitation method") is by far the most commonly used technique for measuring impedance in electrochemical systems. In case (iv.) the multisine signal is the sum of a number of harmonically related sinusoids with freely adjustable amplitudes and phases.

In electrochemistry, the marginal perturbation from equilibrium (or from steady-state) by low amplitude (usually $\leq$ 5–10 mV) sinusoidal voltage is an evident advantage of EIS compared to other techniques involving large-signal perturbations (e.g., chronoamperometry). Although there are several variations, usually an alternating voltage [Eq. (1)]:

$$U(t) = U_m \cos(\omega t) \tag{1}$$

is applied to an electrode and in the physical regime where non-linear effects can be neglected, the resulting current response [Eq. (2)]:

$$I(t) = I_m \cos(\omega t - \varphi) \tag{2}$$

is measured, where ω is the angular frequency ($\omega = 2\pi f$, where f is the frequency) of the sinusoidal potential perturbation, φ is the phase shift between the potential and the current, and U_m and I_m are the amplitudes of the sinusoidal voltage and current, respectively. Of course, an alternating current signal can also be used as perturbation, in this case the resulting voltage response is measured. Irrespective of which technique is used, for systems fulfilling the conditions of linearity, causality, and stability, the calculated impedance values will be exactly the same.

Relations (1) and (2) can be combined into a single linear relation by expressing the voltage and current as the real parts of complex quantities [Eqs. (3) and (4)]:

$$\hat{U}(t) = \hat{U}_m \exp(i\omega t) \tag{3}$$

$$\hat{I}(t) = \hat{I}_m \exp(i\omega t) \tag{4}$$

with $\hat{U}_m = U_m$ and $\hat{I}_m = I_m \exp(-i\varphi)$, where i is the imaginary unit: $i = (-1)^{1/2}$.

The impedance (Z) can be defined as the ratio of the complex voltage and current amplitudes [Eq. (5)]:

$$Z = \frac{\hat{U}_m}{\hat{I}_m} = \frac{U_m}{I_m} \exp(i\varphi) \tag{5}$$

Note that although the impedance is usually complex, we do not put a "hat" on Z. Eq. (5) means that the complex voltage and current obey the linear relation $\hat{U} = \hat{I} \cdot Z$, which is the complex generalization of Ohm's law $U = I \cdot R$.

The impedance can also be given in the form [Eq. (6)]:

[a] K. J. Szekeres, Dr. S. Vesztergom, Dr. M. Ujvári, Dr. G. G. Láng
Department of Physical Chemistry
Institute of Chemistry
H-1117 Budapest, Pázmány P. s. 1/A, Hungary
E-mail: langgyg@chem.elte.hu

$$Z = |Z|\exp(i\varphi) = |Z|\cos(\varphi) + \mathrm{i}|Z|\sin(\varphi) = Z' + \mathrm{i}Z'' \quad (6)$$

where $|Z| = U_m/I_m$ is the magnitude. Z' and Z'' are the real and imaginary part of Z ("resistance" and "reactance"), respectively. (For the real and imaginary parts Z_R and Z_I symbols are also used.)

The concept of impedance can also be introduced in a more general sense, see e.g., Refs. [15–17].

The response of a physical system to a perturbation may be characterized by a transfer function [Eq. (7)]:

$$T(s) = \frac{L\{U(s)\}}{L\{I(s)\}} \quad (7)$$

where $s = \sigma + \mathrm{i}\omega$ (with real numbers σ and ω) is the Laplace transform variable and $L\{U(s)\}$ and $L\{I(s)\}$ are the Laplace transforms of the voltage vs. time and the current vs. time functions, respectively. In principle, any arbitrary time domain excitation can be used to determine the impedance of the system provided that the excitation is applied, and the response is recorded over a sufficiently long time, i.e. a time long enough to complete the transforms over a requested frequency range.

In case of steady-state sinusoidal perturbation, the transfer function becomes [Eq. (8)]:

$$T(\mathrm{i}\omega) = \frac{F\{U(t)\}}{F\{I(t)\}} = \frac{U(\mathrm{i}\omega)}{I(\mathrm{i}\omega)} \quad (8)$$

where F denotes the Fourier transform and $U(\mathrm{i}\omega)$ and $I(\mathrm{i}\omega)$ are the Fourier transforms of the voltage vs. time and the current vs. time functions. In principle, several linear integral transformations can be used to transform functions from the time domain into the frequency domain,[18] but the most well known and most frequently used transformations are the Fourier transform and the Laplace transform (see Appendix A).

Nevertheless, the "operational impedance", which is defined in the Laplace plane, is not used extensively in electrochemistry, though it is conceptually as powerful as its Fourier plane counterpart. Provided that the system is linear, that causality condition is fulfilled, and that the system is stable over the time of measurement, the transfer function may be identified as an impedance $Z(\mathrm{i}\omega)$.[19] The quantities, $T(\mathrm{i}\omega)$ and $Z(\mathrm{i}\omega)$ are complex quantities containing both magnitude and phase information.

It is frequently emphasized that impedance measurements are nondestructive and relatively cheap. Another advantage of the technique is that impedance sensing gives direct electrical signals and does not require a label or other pre-treatment process. For these reasons it is a widely used technique in sensing technology as well[20–24] (chemical sensors, biological sensors, immunosensors, DNA-sensors, enzyme-based sensors, etc.). It is also often applied in processing and quality control of

Krisztina J. Szekeres received her B.Sc. (2015) and M.Sc. (2017) degrees in Chemistry from Eötvös Loránd University Budapest (Hungary) working on connection of electrochemical and morphological behaviors of conductive polymers supervised by Prof. Dr. Gyözö G. Láng. Currently, she is working on combined usage of conductive and non-conductive polymers to solve various problems as a PhD student in the Láng lab. She spent 6 months in Clarkson University (Potsdam, NY USA) working on magneto-controlled enzyme activity supervised by Prof. Dr. Evgeny Katz.

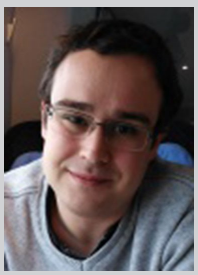

Soma Vesztergom obtained his M.Sc. (2010) and Ph.D. (2014) degrees in Chemistry at Eötvös Loránd University of Budapest (Hungary), as a student of Prof. Dr. Gyözö Láng. He was a post-doctoral researcher in Peter Broekmann's group at the University of Bern (Switzerland) for a year (2014) and remained a regular collaborator of this group since then. His research primarily focuses on instrumental developments in electrochemistry and on the modelling of electrochemical processes (with a particular emphasis on voltammetric measurements in rotating disk electrode systems and electrochemical impedance spectroscopy). Currently, he is an Assistant Professor at Eötvös Loránd University in Budapest.

Maria Ujvari received her M.Sc. (2000) and PhD (2006) degrees in Chemistry from Eötvös Loránd University Budapest (Hungary) working on perchlorate reduction, electrochemical investigation of conductive polymers and partially miscible systems supervised by Prof. Dr. Gyözö G. Láng. Currently, she is working on vanadium redox system, hydrogen evolution and electrochemical characterization of Hantsch-esters – prepared by organic chemistry group – in organic media in the Laboratory of Electrochemistry and Electroanalytical Chemistry as an Assistant Professor.

Gyözö G. Láng received his PhD (CSc) degree in 1991 from Eötvös Loránd University Budapest (Hungary) and the DSc degree in 2004 at the same university. After the PhD, he spent two years at the Technical University Clausthal (Germany) in the group of Prof. K. E. Heusler. In 1998–1999, he was research fellow at the Hokkaido University in Sapporo (Japan) in the group of Prof. M. Seo. His recent research interests include instrumental methods in electrochemistry, electrochemical properties of conducting polymers, metals, and composite materials, thermodynamic and electrochemo-mechanical properties of interfaces, investigation of battery materials, development of electrochemical methods for the treatment of surface and ground water. Currently, he is Full Professor at Eötvös Loránd University Budapest.

foods (meats, milk products, fruits, vegetables, etc..[25,26] Since most biological systems are in fact electrochemical systems, impedance spectroscopy has been adapted as routine technique for the "in situ" study of the interaction of an alternating electrical signal with biological tissue. There are several areas of usage in medical practice as well. For example, mortal prediction in end state kidney failure (ESKF) patients,[27] impedance plethysmography, which is a volume measure method[28–30] or in the detection of pressure-induced tissue damage.[31]

The methods commonly used to interpret impedance data fall into two categories: (i.) analogs and (ii.) physical (physicochemical) models. Analogs, which almost always take the form of electrical equivalent circuits (EECs), do not pretend to describe the electrochemical properties of the system, but simply reproduce the impedance response and hence the information that they can deliver on the physicoelectrochemical processes involved is very limited. In addition, physical significance of the parameters may not always be obvious when data analysis is performed in this manner. On the other hand, physical models should not only reproduce the phenomenon of interest (e.g., the impedance spectrum), but also should also account for the mechanism of the processes occurring at the interface in terms of physicochemically (electrochemically) valid concepts.[32] Consequently, the amount of information that can be gleaned from a full mechanistic analysis far outweighs that which can be obtained by simply fitting the data to ECCs. It should be noted that sometimes the so-called structural approach is employed. The structural approach means that the model structure is derived from experimental data and procedures for parametrical identification are then applied.

As previously mentioned, in electrochemical practice the impedance is measured as a function of frequency. If the "potentiostatic" method is used, a small sinusoidal voltage is superimposed upon the DC polarization potential, and the current is measured. This is perhaps the most popular technique for electrochemical testing in which the AC stimulus level is usually about 5–10 mV. In the "galvanostatic" case a sinusoidal current is superimposed on the DC polarization current and the voltage response is recorded. Under appropriate conditions, that is, at properly selected cell geometry, working and auxiliary electrodes and so on, the impedance response will be related to the properties of the working electrode and the uncompensated (ohmic) resistance between the working and the reference electrodes. Assuming ideal single-sine perturbation, the excitation signal is time-invariant and deterministic. When this method is employed the system under test is sequentially excited by applying small sinusoidal waves of voltage or current within a given frequency range (e.g. from some mHz to some MHz). However, when data recording occurs at low frequencies, a complete measurement sequence can take at least several minutes. From this point of view, it should be taken into account that many electrochemical systems (including biological, reacting, and corroding systems) are intrinsically non-stationary and are affected by time-dependent phenomena.[33] This may be a serious problem since according to the traditional interpretation impedance is not defined as a time-dependent quantity and, therefore, there should not exist an impedance out of stationary conditions. This means that if the requirement of stationarity (stability) during the measurement of "impedance" is not fulfilled, the measured data points are not "impedances", the obtained sets of frequency dependent data points are not "impedance spectra" and their use in any analysis based on traditional impedance models is very questionable. Ignoring this issue may lead to serious problems and confusion, or even to misinterpretation of the experimental data.

In this study we have surveyed the methods of practical use which have been proposed in the literature for dealing with the non-stationarity problem. Selected techniques for the determination of instantaneous impedance spectra in non-stationary systems are briefly reviewed. To better understand the theoretical background of the different approaches, basic principles of the measuring methods and the fundamentals of data collection, validation and correction are also discussed.

2. Measuring Methods, Fundamentals of Data Collection, Validation, and Correction

2.1. Standard Technique of EIS Measurements: Frequency Response Analysis

Electrochemical impedance spectroscopy (EIS) is usually applied for studying stationary systems. A typical scenario of an EIS experiment calls for the application of a small-signal sinusoid perturbation of either the (otherwise stationary) current or the potential of an electrode. In case of potential perturbation, the current response, in case of current perturbation, the voltage response is measured. Ideally, during an impedance measurement both signals are composed of a single sinusoid superimposed on a steady DC component, and a frequency response analyzer (FRA)[34] is used to determine the voltage and current phasors (i.e., complex quantities, that carry information regarding the amplitude and phase of the given sinusoid). It is then possible to calculate the admittance or the impedance by dividing the current and voltage or, respectively, the voltage and current phasors. In FRAs, phasors are determined by multiplying the measured signal with a cosine and a sine wave reference, having the same frequency of the exciting signal. The resulting signal is then integrated over a whole number of cycles of the reference wave, yielding a response that is proportional to the real and the imaginary parts of the phasor (Figure 1). The beauty of FRAs is that all these manipulations can be carried out by using analogue circuitry, using an excitation signal source of programmable amplitude and frequency (the latter is typically between the mHz and the MHz range).

In a noisy environment, the accuracy of FRA-based impedance measurements can be significantly improved by making more than one signal cycles subject to integration. Integration tends to cancel out random noise and also other disturbing components of the measured signals, and longer

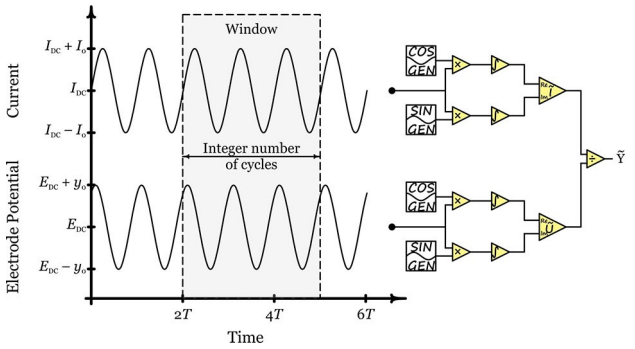

Figure 1. In an FRA, admittance is determined based on the method of sine wave correlation. The voltage and current signals are multiplied by an in-phase (cosine) and a quadrature (sine) reference signal. The frequencies of both reference signals are the same as that used for excitation. Multiplied signals are then integrated over an integer number of cycles to yield the real and imaginary parts of the current and voltage phasors. Admittance (or impedance) is then available by a division of the two complex quantities.

integration times can greatly improve the precision of sine wave correlation, as shown in Figure 2.

Note, however, that increasing the (necessarily integer) number of integrations is possible only at a certain expense of time – thus, in case when the system is unstable on a longer time range, FRAs are only of limited use. In case of a system that only slowly changes with time, recording impedance spectra using FRAs may still be expedient; however, the time dependence of the recorded spectra will then have to be analyzed. This usually necessitates the application of the 4D analysis method originally developed by Stoynov,[35] and further discussed by other authors[36] (see also later in this work).

For systems that are expected to change during the course of measurement of a single point of their impedance spectra, other techniques have to be applied. The most commonly applied such method is based on Fourier transformation (FT). The essence of FT methods is that while a well-composed excitation signal is applied to either the voltage or the current

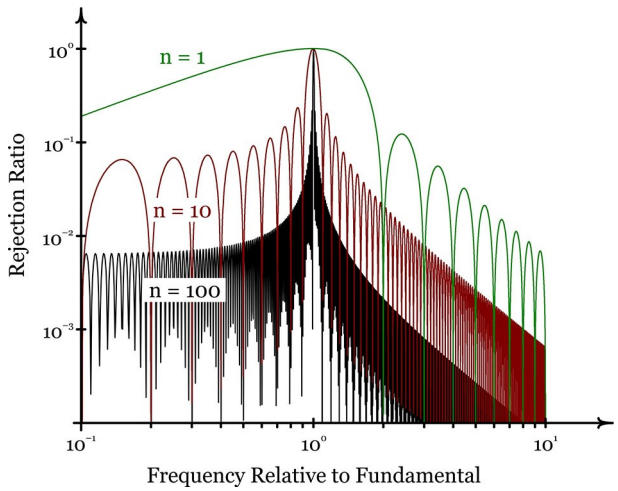

Figure 2. The rejection ratio of sine wave correlators tends to improve as more cycles (*n*) are made subject to integration.

of an electrode, the voltage and current signals are measured back by high precision analog-to-digital converters (ADCs) operated at a suitably high sampling rate. The used ADCs must either be synchronized or a phase correction (*resampling*) is to be made, so that simultaneous digital waveform representations of both the measured current and the measured potential would become available. Phasors of voltage and current, corresponding to a frequency f are then calculated digitally approximating the integrals [Eqs. (9) and (10)]:

$$\hat{U}(f) = \int_{-\infty}^{\infty} U(t) \cdot e^{-2\pi f i t} dt \tag{9}$$

$$\hat{I}(f) = \int_{-\infty}^{\infty} I(t) \cdot e^{-2\pi f i t} dt, \tag{10}$$

and the ratio of the two complex quantities determine the impedance at a given frequency. To carry out these calculations on acquired digital waveforms of potential and current, algorithms such as the fast Fourier transformation (FFT) or the direct Fourier transformation (DFT) can be used; libraries containing these algorithms are available in most programming languages.

FT methods allow the use of not just one but several perturbing frequencies that can even be superimposed on a non-steady baseline (such as on the triangular controlling waveform of cyclic voltammetry). In order to avoid problems arising from the non-linearity of the studied system, multi-frequency perturbation (MFP) usually applies a series of odd, or even prime harmonics. An advantage of MFP is that it can significantly reduce the time needed for impedance measurements. During the time required for measuring the lowest frequency cycle, an integer number of the other, higher frequency cycles can be measured, thus it is the lowest measured frequency alone that limits measurement time. The application of white noise as a perturbing signal may be considered as an extremism of the MFP approach. White noise is a signal that contains a continuous spectrum of frequencies with flat amplitudes. However, single-frequency components have quite low amplitudes, and the response to individual frequencies is also weak, often resulting in rather noisy spectra.

It is clear from the above that the application of FT methods can significantly reduce the time of spectrum acquisition; however, care must still be taken when FT methods are applied for systems with inherent instabilities. As these problems are also present when single-frequency sinusoid perturbations are applied, in what follows we will limit our attention to such single-frequency measurements.

There are two most common kinds of inherent instabilities in electrochemical systems: (i.) when the acquired potential or current waveforms are *drifting* (i.e., a sinusoid of constant amplitude and phase is superimposed on a slowly changing, often non-periodic baseline); and (ii.) when the impedance of the system is itself time dependent, resulting in *enveloped* (often damped) response waves.

2.2. Diagnosing system instabilities using Lissajous plots

For diagnosing the afore-mentioned instabilities, close inspection of the measured signals (on the time domain) or the construction of Lissajous curves (current vs. potential plots) is recommended (Figure 3). Plotting the potential and current signals of an electrochemical cell as a function of time during impedance measurements is possible by using a two-channel oscilloscope (preferably, with AC coupling) equipped to the output signals of the potentiostat. Visually, the creation of Lissajous curves (by using the XY display mode) aids more in detecting system instability. In case of stable waveforms, the Lissajous curves form a motionless oval as in Figure 3(b); while baseline drifting (Figure 3(d)) and amplitude changes (Figure 3(e)) can easily be tracked as effects that cause disturbances that may either remain present or fade away with time. In some commercially available instruments, the creation of Lissajous curves is available in software, making this handy tool available even without the use of an external oscilloscope.

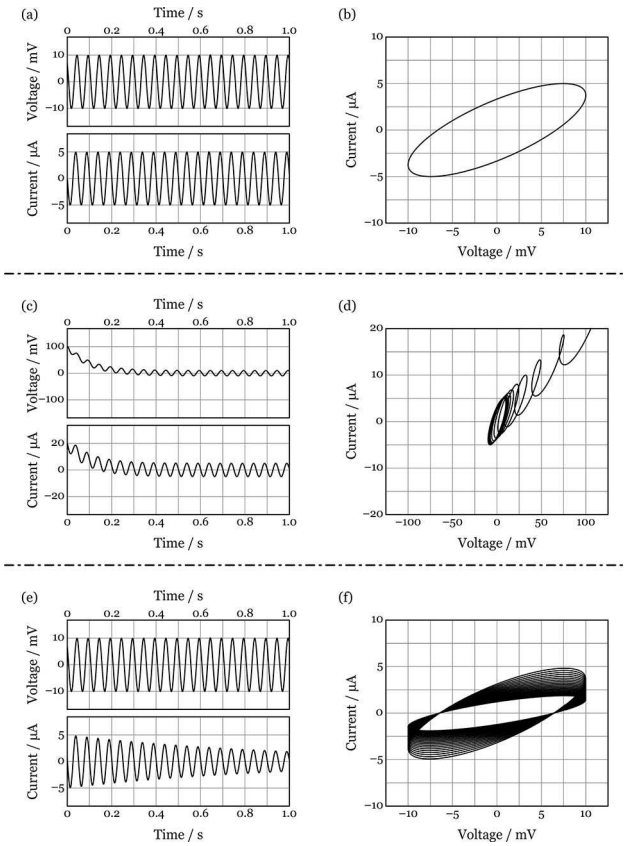

Figure 3. Voltage and current waveforms containing a 20 Hz sinusoid component of 5 mV and, respectively, 5 μA amplitude on the time domain (a, c, e) and the corresponding Lissajous curves (b, d, f). The current lags the voltage by a 40° phase. In (a, b) both the voltage and the current signals are composed of pure sinusoids. In (c) and (d), the voltage and the current sinusoids are superimposed on a slowly changing (drifting) baseline. In (e) and (f), the voltage is a pure sinusoid; the amplitude of the current response, however, slowly decreases with time.

2.3. Diagnosing System Instabilities using Kramers-Kronig Transformations

In accordance with the notation used in the "Introduction", the impedance Z of an electrochemical system is a complex function of the frequency ω [Eq. (11)]:

$$Z(\omega) = Z'(\omega) + \mathrm{i}\,Z''(\omega) \tag{11}$$

where Z' and Z'' represent the real and imaginary parts of impedance, respectively. When ω is real and positive (i.e. when the driving voltage is $U_0 e^{i\omega t}$), then the real part of Z is called the resistance and the imaginary part is called the reactance. We can also imagine cases where ω is complex,[37,38] when the driving force has a real exponential time factor, so that we can consider the immittance function ($Z(\omega)$ or $Y(\omega)$) to be an analytic function of the complex variable ω, and the methods of the theory of functions of a complex variable can be used for the derivation of specific relations which correspond to the Kramers-Kronig relations derived for a general transfer function. In most physically attainable cases Z is analytic in the upper half plane for the complex frequency (i.e., when the imaginary part of ω is positive). The nature of the impedance is such that, if we reverse the sign of ω, the resistance does not change, but the reactance changes sign.

According to the theory of transfer functions, certain relations can be established between the real and imaginary parts, $R(\omega)$ and $X(\omega)$ respectively, of a function [Eq. (12)]:

$$H(\omega) = R(\omega) + \mathrm{i}X(\omega) \tag{12}$$

which arise when $H(\omega)$ is the Fourier transform of a causal function $h(t)$.[39] For instance, it can be shown that if $h(t)$ possesses no singularity at $t = 0$ then [Eq. (13)]:

$$X(\omega) = -\frac{1}{\pi}\int_{-\infty}^{\infty}\frac{R(\omega_1)}{\omega-\omega_1}\mathrm{d}\omega_1 \tag{13}$$

or [Eq. (14)]:

$$X(\omega) = -\frac{2}{\pi}\int_{0}^{\infty}\int_{0}^{\infty}R(\omega_1)\cos\omega_1 t\sin\omega t\,\mathrm{d}\omega_1\mathrm{d}t \tag{14}$$

and [Eq. (15)]:

$$R(\omega) = \frac{1}{\pi}\int_{-\infty}^{\infty}\frac{X(\omega_1)}{\omega-\omega_1}\,\mathrm{d}\omega_1 \tag{15}$$

or [Eq. (16)]:

$$R(\omega) = -\frac{2}{\pi}\int_{0}^{\infty}\int_{0}^{\infty}X(\omega_1)\,sin\,\omega_1 t\,cos\,\omega t\,\mathrm{d}\omega_1\mathrm{d}t \tag{16}$$

Equations (13) and (15) are known as the Kramers-Kronig dispersion relations when they are applied to the scattering of radiation from atomic systems; in this context they imply a relation between the real part of the refractive index and the attenuation in a medium. In the context of servo-mechanisms they are often known as Bode's relations. In a mathematical context transforms of the type introduced in Eqs. (13) and (15) are known as Hilbert transforms (or Kramers-Kronig (K-K) transforms). The Hilbert transform $HT(x)$ of a function $f(x)$ is defined as Eq. (17):[40]

$$HT(x) = \frac{1}{\pi}\int_{-\infty}^{\infty}\frac{f(x_1)}{x_1 - x}\mathrm{d}x_1 \tag{17}$$

The divergence at $x = x_1$ is allowed for by taking the Cauchy principal value of the integral $HT(x) = \frac{1}{\pi}P\int_{-\infty}^{\infty}\frac{f(x_1)}{x_1 - x}\mathrm{d}x_1$ (see Appendix B).

For example, starting from the impedance function of an electrochemical system, we can define an auxiliary function $z(\omega)$ [Eq. (18)]:

$$z(\omega) = Z(\omega) - Z_\infty - \mathrm{i}\chi/\omega \tag{18}$$

where the (real) constants Z_∞ and χ are independent of the angular frequency.[41] It is easy to see that the $z(\omega)$ function defined in the above manner possesses the following properties: $z(\omega)\to 0$ as $\omega\to\infty$ and $z(\omega)$ is well behaved near $\omega = 0$. For an electrode where Faradaic reactions can occur, $\chi = 0$. On the other hand, for an ideally polarizable or blocked electrode $\chi = -1/C$, where C stands for the capacity of the electrode, for instance, it is the double layer capacity. At high values of the frequency, $Z' \to Z_\infty$, where Z_∞ is the uncompensated ohmic resistance of the system, e.g. in an electrochemical system the resistance of the solution, the connections, wires etc.

On the basis of the above considerations, we can conclude that the resulting expressions for the $z(\omega)$ function are [Eqs. (19) and (20)]:

$$Z'(\omega) = Z'(\infty) - \frac{1}{\pi}\mathrm{P}\int_{-\infty}^{\infty}\frac{Z''(\omega_1) - \frac{\chi}{\omega_1}}{\omega_1 - \omega}\mathrm{d}\omega_1 \tag{19}$$

$$Z''(\omega) = \frac{1}{\pi}\mathrm{P}\int_{-\infty}^{\infty}\frac{Z'(\omega_1) - Z'(\infty)}{\omega_1 - \omega}\mathrm{d}\omega_1 + \frac{\chi}{\omega} \tag{20}$$

Or [Eqs. (21) and (22)]:

$$Z'(\omega) - Z'(\infty) = -\frac{2}{\pi}\mathrm{P}\int_{-\infty}^{\infty}\frac{\omega_1 Z''(\omega_1)}{\omega_1^2 - \omega^2}\mathrm{d}\omega_1 \tag{21}$$

$$Z''(\omega) = \frac{2\omega}{\pi}\mathrm{P}\int_{-\infty}^{\infty}\frac{Z'(\omega_1) - Z'(\infty)}{\omega_1^2 - \omega^2}\mathrm{d}\omega_1 + \frac{\chi}{\omega} \tag{22}$$

As it has been shown e.g. in Ref. [37] other sets of similar relations between real and imaginary components of network functions can be derived.

According to Ref. [19] the K-K transforms of interest in analyzing impedance data measured in electrochemical systems are [Eqs. (23)–(27)]:

$$Z'(\omega) - Z'(\infty) = \frac{2}{\pi}\int_0^{\infty}\frac{\omega_1 Z''(\omega_1) - \omega Z''(\omega)}{\omega_1^2 - \omega^2}\mathrm{d}\omega_1 \tag{23}$$

$$Z'(\omega) - Z'(0) = \frac{2\omega}{\pi}\int_0^{\infty}\left[\frac{\omega}{\omega_1}Z''(\omega_1) - Z''(\omega)\right]\frac{1}{\omega_1^2 - \omega^2}\mathrm{d}\omega_1 \tag{24}$$

$$Z''(\omega) = -\frac{2\omega}{\pi}\mathrm{P}\int_0^{\infty}\frac{Z'(\omega_1) - Z'(\infty)}{\omega_1^2 - \omega^2}\mathrm{d}\omega_1 \tag{25}$$

$$\varphi(\omega) = \frac{2\omega}{\pi}\int_0^{\infty}\frac{\log|Z(\omega_1)|}{\omega_1^2 - \omega^2}\mathrm{d}\omega_1 \tag{26}$$

$$R_\mathrm{p} = \frac{2}{\pi}\int_0^{\infty}\frac{Z''(\omega_1)}{\omega_1}\mathrm{d}\omega_1 = Z'(0) - Z'(\infty) \tag{27}$$

where $\varphi(\omega)$ is the phase angle and R_p the polarization resistance.

The derivation of the Kramers-Kronig transforms is based upon four quite general conditions of the system being fulfilled. If these conditions are satisfied, the K-K transforms are purely mathematical results, and do not reflect any other physical property or assumptions concerning the physical properties of the system. The use of the Hilbert Transform (Kramers-Kronig Transform) is model independent. It relies on a mathematical relationship which must exist between the two components of an immittance function for a physically realizable system. Therefore, it can be used in the evaluation of the validity of the data free of any assumptions concerning mechanisms or models.

The usefulness of the Hilbert and Kramers-Kronig transforms in the processing of EIS data was underlined in several publications, e.g. in Refs. [42–46]. In Ref. [47] a general proof was given that the real and imaginary parts of a network function representing a physically realizable network with a distribution of relaxation times satisfy the K-K relations. Some interesting innovations in the field are discussed in.[48–50]

The transfer function constitutes a valid impedance provided that the following criteria are met (it should be noted here, that the terminology used by different authors is far from being consistent, and even the number and meaning of the

necessary conditions that need to be met varies in different literature sources, see e.g. the survey in ref. [51], where an elegant mathematical foundation for validity tests of impedance data and of impedance-based modeling approach by means of mathematical system theory is presented):

2.3.1. Causality

The response of the system must be determined entirely by the perturbation applied and does not contain components from spurious sources. This means that, in the study of two related physical quantities, it should be possible to point out a cause-and-effect relationship between them. More specifically for electrochemical systems, this implies that e.g. the externally applied voltage can be considered as causing the current, or, if current is flowing in a system, a potential difference is built up which can be considered as being caused by the current.[52]

2.3.2. Linearity

The perturbation/response characteristics of the system must be described by a series of linear differential equations. This means that only the first-order term must be present in the response signal. Practically, this condition requires the transfer function to be independent of the magnitude of the perturbation. In the case of electrochemical systems, which are inherently non-linear, this condition is only met if small perturbation amplitudes, e.g., $\Delta U < RT/F$ are used.

2.3.3. Stability

Once the perturbation has been removed the system must return to its original state, i.e. the system may not change with time, nor continue to oscillate when the excitation signal is removed, which requires the system to be passive.

Note, that in the present context the term "stable" is used for systems exhibiting the so-called "asymptotically stable state". Stability usually concerns the response of the interface to a small perturbing signal. However, it depends on both the intrinsic interface dynamics and characteristics of the regulating device. It means that stability refers to the behavior of the whole system. As it has been pointed out in,[53] the term "stable" is sometimes confused with the existence of a steady-state, i.e. conditions that the system does not evolve during the experiment. In terminology of the theory of stability, two types of stability can be distinguished. If the response vanishes with time after withdrawing the perturbation, the system is called asymptotically stable. Conversely, if the response does not vanish but remains bounded (e.g., an oscillation is maintained), the system is called stable. If the system diverges from the steady-state when a perturbing signal is applied, the system is considered unstable.

2.3.4. Continuity and Finiteness

The impedance must be finite-valued and continuous over the frequency range $0 < \omega < \infty$. In particular, the impedance must be tending to a constant real value as $\omega \to 0$ and $\omega \to \infty$. However, for practical application of the K-K transforms this last condition is not critical (see later).

Immittance data which do not Hilbert transform correctly are obtained from a system which does not satisfy the four conditions, and the data may be rejected without further analysis. In principle, the validation of the impedance spectra can be executed by using Kramers-Kronig (K-K) or Hilbert transformations as described e.g., in Refs. [54–57]. As it has been shown in Refs. [58–60] the K-K transforms apparently are especially sensitive to violation of the stability constraint (i.e., to non-stationarity). Some peculiarities of the validation of resonant-type immittance data with KK transformation have been discussed in.[61]

On the other hand, in a recent work it has been demonstrated that application of the Kramers-Kronig relations to the results of multi-sine measurements cannot be used to determine whether the experimental system satisfies the conditions of linearity, causality and stability.[62]

Nevertheless, correct Hilbert (or K-K) transformation of the data is a *necessary but not sufficient* condition to ensure that the system has satisfied the above mentioned four criteria and does not guarantee the validity of the data, but it can increase our confidence in their correctness.

According to the above, failure of Kramers-Kronig test usually means that no good fit can be obtained using the equivalent circuit method.[63,64] On the other hand, it should be noted that the use of complex non-linear regression to analyze immittance data should also verify adherence to the required conditions because the models used in the fitting process themselves satisfy the conditions. The limitation of non-linear regression is that it is model dependent.[65] If the model (analog) is correct and the data are in fact valid, then a good fit will result, and the residuals will contain only random noise. Consequently, a good fit to the data with a physically realistic model will ensure the validity of the data to the same extent that correct K-K transformation would. If the model (analog) is incorrect but the data are still valid, the fit will be unsatisfactory. Conversely, if the model (analog) is correct but the data are invalid, then the fit will also be unsatisfactory. The difficulty arises in attributing the poor fitting results correctly to either the model or the data. K-K transformation would be useful in this situation because of its model independence. With non-linear regression there is also the same question regarding the degree of sensitivity to violations of the four conditions.

It is known that there are some issues in applying KK testing techniques for the validation of measured impedance data. One of them is that the KK transform is strictly defined within the frequency range from 0 to ∞ (see above), whereas the measurements can obviously be performed in a finite frequency range ("limited bandwidth"). This means, that extrapolation of the measured data is inevitable. Some numerical techniques

have been proposed in the past to overcome these problems.[55,66,67]

A feasible method for the validation of experimentally obtained impedance data is the so-called Z-HIT algorithm[68] which involves the evaluation of a "local impedance integral" and therefore avoids extrapolation to the frequencies zero and infinity. Like KK transforms, the Z-HIT method allows the calculation of one component of the transfer function (the impedance modulus) from the other (phase angle).

Alternatives to Kramers-Kronig transformations have been discussed in.[69] A model independent method to calculate the Hilbert Transform of immittance data based on the Fast Fourier Transform (FFT) has been discussed in.[70]

It is worth mentioning that there is a simple experimental way (i.e., without using any mathematical analysis) to check whether the measured data meet the stability requirement or not. During point-by-point impedance measurements the successive impedance values are usually recorded in descending order of frequencies, i.e., from highest to lowest. If the system is time invariant (stationary) reversing the order of frequencies should give the same result. If two measurements (one by decreasing frequency and the 2nd immediately after the 1st by increasing frequency) are performed successively and the results are linked, one can easily see if there are differences between the two sets of data. Systematic deviations indicate that the system under test is time variant.

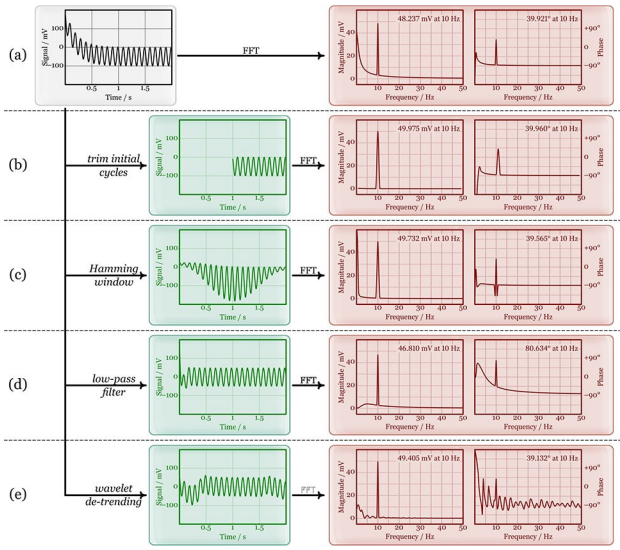

Figure 4. A 10 Hz sinusoid of 40° phase (vs. the cosine function) and 50 mV amplitude is superimposed on a drifting baseline. The baseline starts from 250 mV and decays exponentially with a time constant of 200 ms to a DC voltage of −50 mV. In (a), the magnitude and phase spectra of the waveform are calculated by the FFT algorithm of LabVIEW. In (b), initial cycles are trimmed and only the swung-in state is made subject to FFT. In (c), a Hamming window is applied to the signal before Fourier transformation. In (d), a high-pass filter (Butterworth filter with a threshold frequency of 5 Hz) is applied to the waveform before FFT. In (e), wavelet detrending (with a threshold frequency of 1 Hz) is used to remove baseline drift. Main (10 Hz) components of the magnitude/phase spectra are displayed in the respective graphs.

2.4. Correction for System Instabilities Caused by Baseline Drift

Several modifications of the standard Fourier transformation exist, which allow the determination of the amplitude and the phase of a sinusoid voltage or current waveform that is superimposed on a changing baseline; Figure 4 shows a comparison of these.

As shown in Figure 4(a), applying Fourier transformation directly to the measured waveform leads to heavily distorted magnitude-phase spectra that contain significant drift-originated contributions in the low frequency range. These cause a relatively big error in the determination of the main spectrum component, especially if the applied perturbation frequency and the time constant of baseline drift are comparable. If, like in Figure 4, the baseline drift quickly fades away, there is the possibility of applying the FFT only after a certain number of cycles are recorded, and several potentiostat manufacturers offer this option in their measurement automation software.[71] Trimming the initial, drift-affected cycles leads to better spectra, but the option cannot be used for non-fading baselines (like it is always the case, for example, with dynamic impedance spectroscopy, where EIS measurements are superimposed, e.g., on the control waveforms of cyclic voltammetry).

Apart from trimming, a further available route in overcoming transient effects when Fourier transforming signals distorted by a drifting baseline is to apply windowing.[72] That is, before being made subject to FFT, the signal is multiplied by a typically bell-shaped "window function" that has non-zero values only over a certain closed interval. Windows applied for the purpose of EIS may either be symmetrical or asymmetrical. The latter window functions may be fine-tuned to specifically reject certain types of baseline distortions, but in simple cases like in Figure 4(c), even the application of symmetric windows helps a lot. Here, a Hamming window[73] was applied to the recorded waveform.

Although their use is not recommended for the drift correction of recorded EIS spectra, Figure 4(d) shows an example for the filtering of the recorded signal on the time domain. In this case, the applied filter is a (digital) high-pass Butterworth filter[74] that practically removes all signal components under a certain threshold frequency (in case of Figure 4(d), the threshold frequency is 5 Hz. As can be seen, the obtained signal magnitude is close to the one applied for perturbation, however there is a significant error in the phase. Figure 4(d) thus demonstrates an important caveat of (both digital and, for that matter, analog) filtering: namely that filters always introduce a significant phase shift to the recorded waveforms. In electrochemical instrumentation it is easy to avoid digital filtering, analog filters are however almost always used in modern EIS measurements. The reason is that the AC components of the measured signals must be efficiently decoupled, and then amplified to be monitored by ADC samplers. The main message of Figure 4(d) is thus very important from the point of view of instrumentation: that is, when carrying out impedance measurements, care must be taken that either no filters are used, or the same filters are

applied to both the recorded voltage and the current, even if some of these waveforms may look unaffected by drift, not requiring filtering. When a drifting baseline is to be removed digitally, de-trending algorithms based on the method of discrete wavelet transformation[75] (like those included in LabVIEW) usually prove more effective than most digital filters, and by their use the appearance of spurious phase shifts may be avoided.[76]

In case of more drastically changing baselines, the calculation of rotating Fourier transforms, as proposed by Stoynov,[77] may be successfully applied to recover the perturbing amplitude and phase. Provided that $y(t)$ is a measured signal, its phase definite Fourier transform (PFT, a name coined by Stoynov) can be calculated, using numerical integration, at frequency f as Eq. (28):

$$\mathrm{PFT}(f) = \frac{2}{nT}\int_{\tau}^{\tau+nT} y(t)\cdot \mathrm{e}^{-2\pi f \mathrm{i} t}\mathrm{d}t, \tag{28}$$

Integration in the above equation is to be carried out using a time window of length $n\ T$ that contains exactly n integer periods of the applied perturbing waveform (of period T). For a signal that consists not only of a single sinusoid, but also an additional drifting baseline, the integration may yield different results, depending on the τ initial time of integration. This is what makes the transformation phase (i.e., initial time) definite.

Provided that we choose different τ values lying between 0 and $k\ T$ as starting times of the integration (k is also an integer), the expected value of the above integral may be calculated in the form of the following time average [Eq. (29)]:

$$\mathrm{RFT}(f) = \frac{2}{nkT^2}\int_{0}^{kT}\int_{\tau}^{\tau+nT} U(t)\cdot \mathrm{e}^{-2\pi f \mathrm{i} t}\mathrm{d}t\mathrm{d}\tau \tag{29}$$

The above selection for the integration limits of τ makes it possible to interpret (the outer) integral as an integration by phase. Since the initial phase rotates an integer number of periods, Stoynov called this transformation a rotating Fourier transform (RFT).[77] In his paper[77] Stoynov showed that the simple RFT (as defined by eq.(29)) is already orthogonal to any first-order (linear) terms of the noise spectrum. E.g., it can be seen that for a signal of the form [Eq. (30)]:

$$U(t) = A\cos(2\pi f_0 t + \varphi) + bt + c, \tag{30}$$

that is, a sinusoid superimposed on a linear trend, the corresponding RFT is [Eq. (31)]:

$$\mathrm{RFT}(f) = \frac{2Af^2\sin^2\left(\pi\frac{f_0}{f}\right)}{(f^2+f_0^2)^2\pi^2}\begin{bmatrix}\left(f^2+f_0^2\right)\cos\left(2\pi\frac{f_0}{f}+\varphi\right)\\ +2\mathrm{i}\,f\,f_0\sin\left(2\pi\frac{f_0}{f}+\varphi\right)\end{bmatrix}, \tag{31}$$

that in case of $f \to f_0$ simplifies to [Eq. (32)]:

$$\mathrm{RFT}(f_0) = A\mathrm{e}^{\mathrm{i}\varphi}. \tag{32}$$

However, in Ref. [77] Stoynov already generalized Equation (29) to an expression that accounts for disturbances of higher order. (Unfortunately, this has not facilitated a better understanding.)

According to Stoynov, a rotating Fourier transformation of order m can be described by the following formula [Eq. (33)]:

$$\mathrm{RFT}_m(f) = \frac{2}{nT^{m+1}\prod_{i=1}^{m}k_i}\int_0^{k_mT}\cdots\int_0^{k_1T}\int_{\sum_{i=1}^{m}\tau_i}^{\sum_{i=1}^{m}\tau_i+nT} U(t)\cdot\mathrm{e}^{-2\pi f\mathrm{i}t}\mathrm{d}t\mathrm{d}\tau_1\mathrm{d}\tau_m\ , \tag{33}$$

that is, by calculating more than one time averages. The method of Stoynov proved exceptionally useful for the recovery of small signal perturbation characteristics superimposed on quickly changing baselines. As shown in Figure 5, an m order RFT yields a perfect estimate for the magnitude and phase of a sinusoid added to an m order polynomial. While for more erratic baselines higher order RFTs ($m=3$ or 4) may have to be applied, the method of rotating Fourier transformation provides excellent means for drift rejection during electrochemical impedance measurements.

3. Systems of Time-Dependent AC Response

In case, however, when not only the baseline is drifting but (as was shown, for example, in Figure 3) also the AC response is subject to temporal changes, other methods have to be applied to determine the time dependence of impedance spectra. One convenient possibility of determining time-varying impedances is by the construction of generalized spectrograms, as shown in Figure 6. The definition of the spectrogram relies on Gábor transform, described in 1946 by the Hungarian Nobel laureate Dénes Gábor.[78,79] A sub-class of short-time Fourier transforms (STFTs),[80] the Gábor transform is used to retrieve the amplitude and phase content of local sections of a signal at different frequencies, as the signal changes with time. The measured

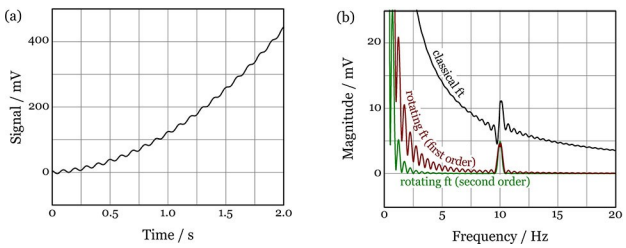

Figure 5. A 10 Hz sinusoid of 20° phase (vs. the cosine function) and 5 mV amplitude is superimposed on a rapidly changing, second-order baseline ($100\ \mathrm{mV\,s^{-2}}\ t^2 + 20\ \mathrm{mV\,s^{-1}}\ t$) (a). Magnitude spectra of the waveform prepared by classical Fourier transformation, as well as by 1st and 2nd order rotating Fourier transformation (b).

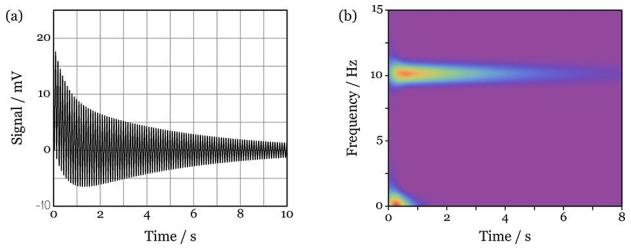

Figure 6. An example of time-dependent response: a 10 Hz sinusoid waveform enveloped by an exponential decay of 5 s time constant, superimposed on a drifting baseline that also decays exponentially, with a time constant of 500 ms (a). The corresponding Gábor spectrogram, prepared by LabVIEW's Time Frequency Analysis Toolkit (b), decouples the decaying 10 Hz component from the other (low frequency) components.

signal is first multiplied by a Gaussian function, which can be regarded as a window function, and the resulting function is then transformed with a Fourier transform to derive the time-frequency analysis. To show the performance of spectrograms, the time dependent signal in Figure 6(a) was transformed to a time-frequency grid in Figure 6(b), using the algorithm available in the Advanced Signal Processing Toolkit of LabVIEW. As can be seen, time-frequency analysis based on Gábor spectrograms provide excellent means for studying the time dependence of the AC response of systems.[81] Although not yet available in any commercial EIS analysis software, it is expected that these results of modern digital signal analysis will have a significant future impact on the interpretation of EIS measurements.

4. Selected Methods for the Determination of Instantaneous Impedance Spectra in Non-stationary Systems

4.1. The GAUSSIAN Window

Darowicki et al.[82–85] developed a method to determinate instantaneous impedance spectra by the connection of the pseudo-white noise,[86] and the short-time Fourier transformation (STFT) methods.[87,88] By this coupling, the impedance spectra can be determined as the function of time. The perturbation signal was a package of n sinusoidal voltage signals with the same amplitude but different frequencies. The response of the investigated signal was a package of elementary current components of the same frequency composition. However, phase angles depend on the properties and characteristics of the investigated process. The Fourier transformations of the elementary current signal do not reflect changes in the investigated system in time. In contrast, STFT transformation, which differs from the regular Fourier transform by a term called the Gaussian window, reflects the frequency composition of the perturbation package and the amplitude changes in time, allows determination of the frequency spectrum changes as the function of time. Basically, during the STFT transform a signal portion was cut out by the window with a Gaussian peak shape, and then a regular Fourier transformation was performed. The procedure was carried out in the whole time range, in which the analyzed signal has been recorded. By carrying out a local Fourier transformation for each localized time range determined by the value $\sigma(t)$ (where $\sigma^2(t)$ is the variance of the Gaussian peak in the domain of time), instantaneous power density spectra were obtained. In the case of the stationary signal, there was no time dependence of the obtained power density spectra. When the signal was non-stationary, the dependence of the spectral power density on time becomes evident. By using the method of pseudo-white noise analyzed by the STFT method time-frequency impedance/admittance spectra can be obtained. The frequency resolution and time selectivity of the total time-frequency analysis of impedance/admittance spectra depends on the choice of size of the Gaussian window. However, a drawback of the method is that it is not possible to register the impedance spectra in a wide range of frequencies. See Figure 7.

4.2. Odd Random Phase Multisine with a Random Harmonic Grid

Hubin et al.[89–94] described a measurement method for electrochemical impedance spectroscopy, using specially designed broadband excitation signals. A procedure was proposed to quantify and correct for the time-evolution by means of the calculation of an instantaneous impedance. A multisine composed by odd harmonics of a base frequency, removing every third frequency was employed. The impedance, the level of the disturbing noise, the non-linear distortions, and the non-stationary behavior were measured simultaneously. Using the odd random phase multisine excitation signal (ORP-EIS), they were able to correct the effect of the time-evolution of the system on the impedance spectra. By the acquisition of consecutive data sets, the variation of the impedance with time was reconstructed. However, they needed to assume a particular shape of the time variation of the impedance. The final results were modeled using equivalent circuits.

4.3. Dynamic Multifrequency Analysis

Battistel et al.[95,96] introduced the dynamic multi-frequency analysis (DMFA) and compared it with a set of consecutive

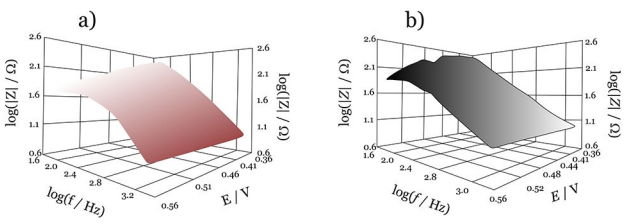

Figure 7. Three-dimensional spectra determined on the basis of a) peak value changes of each frequency peak in the function of polarization and b) of static impedance measurements of the investigated model electrical system. The figures were adapted with permission from Ref. [83]. Copyright (2000) Elsevier. License number: 5024961417529.

stationary impedance spectra on the ground of a simulated system consisting of a redox couple in solution in contact with a platinum electrode. The mathematical formulation of the conciliation of time dependence into the concept of impedance was presented. A new fitting algorithm with the usage of standard equivalent circuits and an algorithm[97] for handling the time variation of the fitting parameters were proposed and tested. During the fitting procedure, the Randles circuit: $R_s + C_h/(R_{ct} + W)$, (where R_s is the resistance of the electrolyte, C_h is the differential interface capacitance, R_{ct} is the charge transfer resistance) was used. C_h was larger in the case of the dynamic impedance and shows a lower variation. The voltage profile of the cyclic voltammetry had a small influence on the value of the double layer capacitance both in stationary and dynamic conditions. The Warburg element (σ) had a minimum in correspondence of $E_{1/2}$ which is influenced by the ratio of the diffusion coefficients of the redox couple, while the minimum of the charge transfer resistance was determined also by the symmetry factor of the reaction. R_{ct} and σ did not overlap either between stationary and dynamic impedance nor between cathodic and anodic scan. See Figure 8.

4.4. Potentiodynamic Electrochemical Impedance Spectroscopy

Ragoisha et al.[98] used the so-called potentiodynamic electrochemical impedance spectroscopy (PDEIS) to investigate the irreversible lead underpotential deposition (upd) on tellurium. The idea of PDEIS bases on the extension of electrochemical impedance spectroscopy (EIS) to use it under non-stationary conditions, similar to cyclic voltammetry (CV). With the usage of potentiodynamic electrochemical impedance spectroscopy 3D picture can be got that characterizes not only the dc current but the potential dependence of the impedance spectra as well. In order to measure a PDEIS spectra of non-stationary systems virtual instruments operating in the real-time mode are needed. It is important to note, that in this case, the frequency range is necessarily narrower compared to the commonly used non-dynamic EIS.

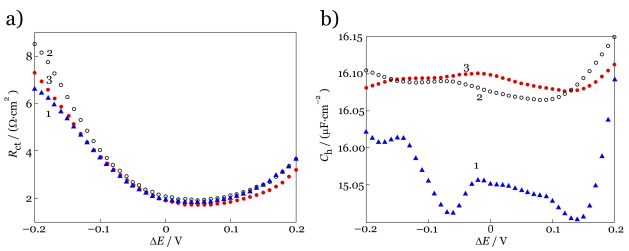

Figure 8. Comparison of a) charge transfer resistance (R_{ct}) and b) double layer capacitance (C_h) derived from the fitting of the static impedance (1) and for the dynamic impedance [cathodic scan (2) and anodic scan (3)]. The figures were adapted with permission from Ref. [95] Copyright (2016) Wiley-VCH. License number: 5024981429616.

4.5. Dynamic Electrochemical Impedance Spectroscopy

Sacci and Harrington[99–101] developed software and hardware for dynamic electrochemical impedance spectroscopy (dEIS), which is a similar method to short-time Fourier Transform (STFT). The system on top of a potential sweep applies a continuous computer-generated small-amplitude multisine waveform. The hardware is compatible with any analog potentiostat since the digitalization of the current and voltage sings takes place in a USB controlled instrument. Advantage of this method, that the impedance spectra can be measured incessantly around a cyclic voltammogram, ergo it is suitable for non-stationary conditions. In addition, when dc and ac signals are generated from separate sources, one can get more freedom in the types of dEIS experiments.

Before the fast-Fourier transform of the measured signals (current and potential), a baseline correction needs to be taken. The impedances can be got by the quotient of the complex transformed potential and current. Dummy cell was used to test the dEIS method, which is usable both steady-state EIS, chronoamperometric EIS, and potential sweep EIS experiments.

4.6. Rotating Fourier Transform

One of the kernels of electrochemical impedance spectroscopy is the Fourier Transform (FT). However, its usage under non-stationary conditions is not recommended, because methodical errors are produced. To solve this problem, Stoynov[77,102,103] developed a new mathematical transform, the so-called Rotating Fourier Transform (RFT), and also showed its first experimental application. The method of Stoynov, described in detail in a previous section, was recommended by Stoynov to be used in corrosion, passivation, AC polarography, or battery studies.

The form of the new transform is [Eq. (34)]:

$$X(i\omega, \psi, N) = \frac{1}{2\pi n_1} \int_{\psi}^{\psi+2\pi n_1} w \, d\varphi \tag{34}$$

where [Eq. (35)]:

$$w = \frac{1}{nT} \int_{t_i}^{t_i+nT} x(t)\, e^{-i\omega t} \, dt \tag{35}$$

where $x(t)$ is the input signal. As it can be seen in Eqs. (34) and (35), the classical integration of the Fourier Transform is spread over an integer number of periods and it rotates n times, in this reason the new name of the transform is "Rotating".

Equation (34) can be generalized further, and Multiple Rotating Transform (MRT) is defined [Eq. (36)]:

$$x^v(i\omega) = \left\{ (2\pi)^v \prod_i^v n_i \right\}^{-1} \times \int_{\psi}^{\psi+2\pi n_v} \dots \int_{\psi_1}^{\psi_1+2\pi n_1} w \, d\varphi \dots d\psi_{v-1} \tag{36}$$

where the order v is orthogonal to all n terms ($n=v$) of the aperiodic noise Taylor spectrum.

Both of the new methods (RFT and MRFT) keep the property of the original Fourier Transform with respect to periodic signals.

It is important to note, that simple back transforms are unable to restore the filtrated initial constant value and its time-derivatives, for that other mathematical tools should be used. The robustness of the RFT was also tested: the variations of the initial phase of a single frequency record was produced impedance results with $\Delta < 0.25^\circ$ phase differences.

The author recommends some electrochemical fields, where RFT method can be used: corrosion, passivation, AC polarography, or measurement of the battery impedance during its operation, but it can be also useful in physics, geophysics, and material science.

4.7. Fast Time-Resolved EIS

Popkirov developed a two-cells measurement method for fast EIS measurements, that can be used under non-stationary conditions.[104] The relaxation component of the response signal is subtracted in real-time. This experimental method uses two identical electrochemical cells (the second one is a reference cell) to eliminate relaxation currents from the response current due to changes in the DC bias voltage.

As the schematic diagram of the measurement set-up (Figure 9) shows, in order to set equal DC conditions for both cells, DC bias voltage ($\bar{U}_{bias}$) is applied to the input terminals of both potentiostats. To avoid phase and amplitude distortions the second potentiostat needs better frequency response, that is the reason for the usage of the perturbation AC voltage ($\tilde{U}_{pert}$) in this case. To get a voltage proportional to the response current ($\tilde{I}_{resp}$) the IC #3 differential amplifier was used. In this way, the relaxation currents can be eliminated from the response current, if both cells are identical.

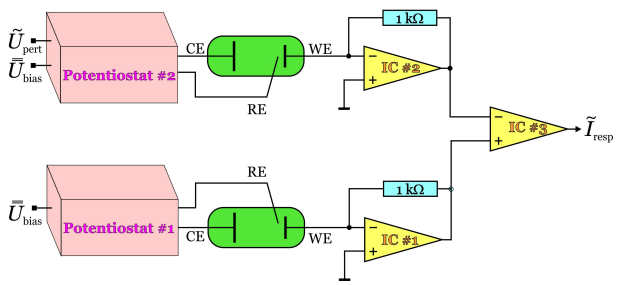

Figure 9. Electronic circuit diagram of the "two-cells experimental technique for fast EIS" measurements set-up. The figure was adapted with permission from Ref. [104] Copyright (1996) Elsevier. License number: 5024970467228.

4.8. Method of Determining Instantaneous Impedance Diagrams for Non-stationary Systems Based on a Four-Dimensional Approach

Stationarity usually refers to a system that exhibits stationary behavior through time. Non-stationarity then refers to something that is changing over time. This means that non-stationary behavior of a system clearly violates the stability criterion for transfer functions. However, it is possible to show that under some suitable conditions time dependence can be conciliated into the concept of impedance. Perhaps the most straightforward (approximative) method is that proposed by Stoynov (and developed further by other authors) for determining (or reconstruction) instantaneous impedance diagrams for non-stationary systems based on a four-dimensional approach.[68,103,105–107] The "instantaneous impedance" is defined as an instantaneous projection of the non-stationary state of the system into the frequency domain. (A related and only slightly different data treatment method can be found in refs. [108,109].)

This post-experimental analytical procedure (the "4-dimensional analysis") provides for correction of the systematic errors, arising during the measurements of time-evolving impedance, i.e. when the consecutive impedance measurements are performed at different system states, but each of the data points obtained at a given frequency can be accepted as "valid" impedances in the classical sense. The method is, in principle, based on the assumption that only insignificant changes in the system occur during the time required for measurement of a single data point, and the measured "impedance spectra" (and not the single data points) are corrupted by errors caused by the system evolution during the experiment.[105,106,110–114] In other words, the errors due to non-stationarity are reflected by the structure of the data and not by the individual data values.

The basis of the four-dimensional analysis method is the assumption that the state space and the parameter space (i.e., the space of possible parameter values that define a particular mathematical model) are continuous. On the other hand, no assumptions concerning the quality or structure of the system under investigation are needed for the application of the method. The application of the method requires the subsequent recording of "impedance" data sets at the same set of frequencies (Figure 10(a)). A data point recorded at a particular test frequency should additionally contain the time information of the measurement (these so-called "timestamps" can be the starting or ending times of the measurements of the individual impedance values, arithmetic or other suitably selected averages, etc.). Thus, the experimental data form a set of 4-dimensional arrays, containing the timestamp, frequency, and the real and imaginary components of the impedance (Figure 10(b),(c)). For every measured frequency two one dimensional functions of "iso-frequency dependencies" (e.g., for the real and for the imaginary components) are constructed. On the basis of the continuity of the evolution, interpolation (and/or extrapolation) is performed (e.g., by using smoothing or interpolating cubic spline or other interpolation functions) resulting in instantaneous projections of the full impedance-

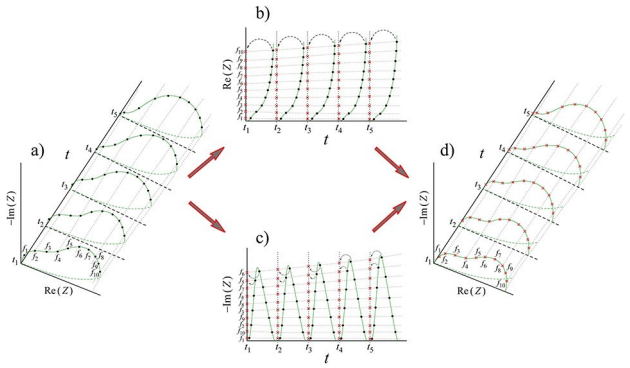

Figure 10. Scheme of the mathematical procedure. a) 3D representation of the impedance and time evolution in Re(Z), −Im(Z) and t coordinates. Re(Z): real part of the complex impedance, Im(Z): imaginary part of the complex impedance, t: time. ●: measured data points (impedances) corresponding to the frequencies f_i, t_i: starting time of the ith frequency scan. b) Iso-frequency dependencies and calculation of the instantaneous (corrected) Re(Z) values (×) by interpolation of the measured Re(Z) data. c) Iso-frequency dependencies and calculation of the instantaneous (corrected) −Im(Z) values by interpolation of the measured Im(Z) data. d) 3D representation of the 'reconstructed' instantaneous impedances related to the beginning of each frequency scan. ×: corrected data points (impedances) corresponding to the frequencies f_i.

time space and "reconstructed" instantaneous impedances related to a selected instant of time (i.e., the beginning of each frequency scan) (Figure 10(d)). Thus, a set of impedance diagrams is obtained, containing instantaneous impedances corresponding to the same time moments. Each of these impedance diagrams can be regarded as stationary, free of non-steady-state errors.

One may conclude from the above considerations that that the four-dimensional analysis method is most effective in the correction of impedance data measured at low frequencies. Whereas this conclusion may be correct, it has recently been shown that the 4-dimensional analysis method is an effectual tool for handling non-stationary data sets recorded at higher frequencies as well.[110,111]

In these studies, the method was successfully applied for the determination of some characteristic impedance parameters of overoxidized gold | poly(3,4-ethylenedioxytiophene) (PEDOT) | sulfuric acid (aq) electrodes. For instance, the charge transfer resistance corresponding to different time moments, including the time instant just after the overoxidation of the polymer film, could be determined, proving that the 4-dimensional analysis method can not only be used for the correction of the actually measured impedance data, but it opens up the possibility of the estimation of the impedance spectra outside the time interval of the measurements. According to the results the so called "low frequency capacitance" or "redox capacitance" of the polymer film is almost time independent. This means that the changes of the impedance spectra with time are solely due to time evolution of the charge transfer resistance and the double layer capacitance at the gold substrate/polymer interface. Consequently, in these cases the high and medium frequency regions of the impedance spectra are stronger affected by the time evolution than the values measured at low frequencies. (It should be noted here that apparently there are no generally accepted standard frequency ranges in electrochemical impedance spectroscopy (EIS). To assist with the interpretation of the EIS data, usually three frequency ranges are identified. These include a "high" frequency range from about 1 kHz up to 1–10 MHz, an "intermediate" (or "medium") frequency range from 1 kHz to 1 Hz (or 0.1 Hz), and a "low" frequency range with frequencies below 1 Hz (or 0.1 Hz). However, the selection (or definition) of the potential ranges may depend on the properties of the system under investigation and the boundaries may be blurred.)

A free installer package of the software presented at the 71st Annual Meeting of ISE[115] for the correction of "impedance" data measured under non-stationary conditions can be downloaded from the following link:[116]

5. Concluding Remarks

Methods based on impedance measurements have been continuously growing in popularity over the past decades. This is not necessarily because of the universal applicability of the technique, but rather because the availability of devices for automated impedance measurements has steadily increased over the same time period. In addition, manufacturers' brochures often suggest that using highly automated equipment the measurements can be carried out routinely with little technical effort, and the evaluation of the measured data can be performed with ease using the included software packages.

Unfortunately, the design of a valid EIS measurement is not trivial in practice as the systems under test also have to meet certain requirements concerning the possibility of measuring true impedance values, and, in particular, true impedance spectra. One of the most underestimated problem lies in the validity of measured "impedance" data. The key ingredient to overcome this problem is to perform the EIS measurement in such way, that certain a priori technical assumptions are fulfilled. However, this is not always possible. One of the most serious problems encountered in the reliable measurement of impedance data is that many electrochemical systems (including biological, reacting, and corroding systems) are intrinsically non-stationary and potentially unstable. The methods proposed for handling such situations include tools and techniques for performing EIS measurements in such way that certain a priori technical requirements are fulfilled as well as post-experimental procedures such as "the 4-dimensional analysis" method.

In the last decades, several methods have been proposed in the literature to handle issues connected with impedance measurements in time-varying (non-stationary) systems, however, the most advanced methods are not commonly implemented. One of the reasons for this underuse could be the methodological complexity of the techniques. Most probably another reason is the lack of adequate software solutions and/or specific guidance concerning the functioning of the software applications.

The purpose of this work was to provide an overview and guidance on some of the practically relevant methodologies

published in the literature to address problems related to impedance measurements in time-varying systems.

Appendix A

Fourier Transform

Fourier transform (FT) is a mathematical transformation that decomposes functions depending on time (or space) into functions depending on frequency (spatial or temporal). The term "Fourier transform" is used for both the frequency domain representation and the mathematical operation that associates the frequency domain representation to a function of time. There are several common conventions for defining the Fourier transform of an integrable function g. One of them can be written in terms of the frequency f or angular frequency ω (the Fourier transform of a function g is traditionally denoted $\hat{g}$, by adding a circumflex to the symbol of the function) [Eq. (A1)]:

$$F\{g(t)\}(\omega) = \hat{g}(\omega) = \int_{-\infty}^{\infty} g(t)\, e^{-i\omega t} dt = \int_{-\infty}^{\infty} g(t)\, e^{-i2\pi ft} dt \tag{A1}$$

A reason for the negative sign in the exponent is that it is common in electrical engineering.

The Fourier Transform of a function can be derived as a special case of a Fourier Series of a function $g(t)$ when the period $T \to \infty$.

Start with the Fourier Series synthesis equation [Eq. (A2)]:

$$g(t) = \sum_{n=-\infty}^{\infty} c_n e^{2\pi i \frac{n}{T} t}, \tag{A2}$$

where the nth series coefficient c_n is given by [Eq. (A3)]:

$$c_n = \frac{1}{T} \int_{-T/2}^{T/2} g(t)\, e^{2\pi i \frac{n}{T} t} dt. \tag{A3}$$

Eq. (A3) can also be written as [Eq. (A4)]:

$$Tc_n = \int_{-T/2}^{T/2} g(t)\, e^{2\pi i \frac{n}{T} t} dt = \int_{-T/2}^{T/2} g(t)\, e^{i n\, \omega_0 t} dt. \tag{A4}$$

Equation (A1) is obtained if $T \to \infty$, $\omega = n\omega_0$ and $\hat{g}(\omega) = Tc_n$.

The integral for the Fourier transform can be studied for complex values of its argument. Depending on the properties of g, this might not converge off the real axis at all, or it might converge to a complex analytic function for all values of [Eq. (A5)]:

$$f = \sigma + i\tau, \tag{A5}$$

or something in between.

Laplace Transform

The Fourier transform is related to the Laplace transform (LT), which is also used e.g., for the solution of differential equations or the analysis of filters. The (unilateral Laplace transform) is defined by [Eq. (A6)]:

$$L\{g(t)\}(s) = \int_{0}^{\infty} g(t)\, e^{-st} dt \tag{A6}$$

where $g(t)$ is defined for $t \geq 0$. The unilateral Laplace transform is almost always what is meant by " Laplace transform", although a bilateral Laplace transform is sometimes also defined as [Eq. (A7)]:

$$L\{g(t)\}(s) = \int_{-\infty}^{\infty} g(t)\, e^{-st} dt. \tag{A7}$$

(for more details see Refs. [117,118]).

Appendix B

Cauchy Principal Value

An integral from minus infinity to plus infinity is usually a limit defined by [Eq. (B1)]:

$$I_1 = \int_{-\infty}^{+\infty} f(x)\, dx = \lim_{\xi_1, \xi_2 \to \infty} \int_{-\xi_1}^{\xi_2} f(x)\, dx \tag{B1}$$

where the quantities ξ_1 and ξ_2 tend to infinity independently of each other. If an improper integral in the above sense is divergent, by introducing $\xi = \xi_1 = \xi_2$ into eq. (B1) the integral can be given a somewhat limited interpretation known as Cauchy principal value, defined by[Eq. (B2)]:

$$I_2 = \mathrm{P} \int_{-\infty}^{+\infty} f(x)\, dx = \lim_{\xi \to \infty} \int_{-\xi}^{\xi} f(x)\, dx \tag{B2}$$

It is possible that the limit (B2) exists, but not that in (B1), e.g. if $f(x) = x$, then I_2 equals zero, but I_1 has no meaning.

In fact, the integral (B2) of all odd functions equals zero, whereas (B1) might not exist. For example, $P \int_{-\infty}^{+\infty} \frac{dx}{x} = 0$.

A similar interpretation applies also for singularities at finite points; if $f(x) \to \infty$ for $x \to x_0$, then the integral of $f(x)$ in an interval (ξ_1, ξ_2) containing x_0 can be defined by [Eq. (B3)]:

$$\int_{\xi_1}^{\xi_2} f(x)\, \mathrm{d}x = \lim_{\varepsilon_1, \varepsilon_2 \to 0} \left[\int_{\xi_1}^{x_0 - \varepsilon_1} f(x)\, \mathrm{d}x + \int_{x_0 - \varepsilon_2}^{\xi_2} f(x)\, \mathrm{d}x \right] \tag{B3}$$

where the quantities ε_1 and ε_2 tend to zero independently of each other. If such a limes does not exist, it is a common usage to define the Cauchy principal value of the integral as [Eq. (B4)]:

$$\mathrm{P}\int_{\xi_1}^{\xi_2} f(x)\,\mathrm{d}x = \lim_{\varepsilon\to 0}\left[\int_{\xi_1}^{x_0-\varepsilon} f(x)\,\mathrm{d}x + \int_{x_0-\varepsilon}^{\xi_2} f(x)\,\mathrm{d}x\right] \tag{B4}$$

For example, the $\int_{-1}^{+1}\frac{\mathrm{d}x}{x}$ integral is divergent, however, $\lim_{\varepsilon\to 0}\left[\int_{-1}^{-\varepsilon}\frac{\mathrm{d}x}{x}+\int_{\varepsilon}^{1}\frac{\mathrm{d}x}{x}\right]=\lim_{\varepsilon\to 0}[0]=0$.

Another, very important example is the integral $I=\int_a^b \frac{\mathrm{d}x}{c-x}$, $a<c<b$.

It is clear, that I has no meaning in the usual sense if ε_1 and ε_2 are independent, since the expression [Eq. (B5)]:

$$\int_a^{c-\varepsilon_1}\frac{\mathrm{d}x}{c-x}+\int_{c+\varepsilon_2}^{b}\frac{\mathrm{d}x}{c-x}=\ln\frac{c-a}{b-c}+\ln\frac{\varepsilon_2}{\varepsilon_1} \tag{B5}$$

is indefinite.

However, with $\varepsilon_1=\varepsilon_2=\varepsilon$ we obtain an expression which is independent on ε [Eq. (B6)]:

$$\int_a^{c-\varepsilon}\frac{\mathrm{d}x}{c-x}+\int_{c+\varepsilon}^{b}\frac{\mathrm{d}x}{c-x}=\ln\frac{c-a}{b-c} \tag{B6}$$

It means, that $P\int_a^b\frac{\mathrm{d}x}{c-x}=\ln\frac{c-a}{b-c}$. In addition, for $a=-b$ (see. eq. (B2)) $\lim_{b\to\infty}\left[\ln\frac{c+b}{b-c}\right]=0$, therefore the following equations are also true [Eq. (B7)]:

$$\mathrm{P}\int_{-\infty}^{+\infty}\frac{\mathrm{d}x}{c-x}=\int_{|x-c|>\delta}\frac{\mathrm{d}x}{c-x}=0. \tag{B7}$$

The Cauchy principal value can also be defined in terms of contour integrals of a complex-valued function [Eq. (B8)]:

$$f(z): z=x+\mathrm{i}y,\ x,y\in\mathbb{R}, \tag{B8}$$

with a pole on a contour C (for more details see Refs. [119–121]).

Let $C(\varepsilon)$ be that same contour, where the portion inside the disk of radius ε around the pole has been removed. Provided the function is integrable over the latter contour (no matter how small ε becomes), then the Cauchy principal value is the limit [Eq. (B9)]:

$$\lim_{\varepsilon\to 0^+}\int_{C(\varepsilon)} f(z)\,dz=\mathrm{P}\int_C f(z)\,dz \tag{B9}$$

In the case of functions which are integrable in absolute value ("Lebesgue-integrable"), the above definition coincides with the standard definition of the integral.

Acknowledgements

Financial support from the National Research, Development, and Innovation Office (NKFIH, grant nos. K129210 and FK135375) is gratefully acknowledged. The work within project no. VEKOP-2.3.2-16-2017-00013 and the ELTE Institutional Excellence Program (TKP2020-IKA-05) was financed by the European Union and the Hungarian Ministry of Human Capacities. The work was also supported by the ÚNKP-20-3 New National Excellence Program of the Ministry for Innovation and Technology from the source of the National Research, Development, and Innovation Fund.

Conflict of Interest

The authors declare no conflict of interest.

Keywords: electrochemical impedance spectroscopy (EIS) · frequency response analysis · Kramers-Kronig transformation · non-stationary conditions · instantaneous impedance

[1] A. J. Bard, L. R. Faulkner, *Electrochemical Methods*, Wiley, New York, **2001**.
[2] U. Retter, H. Lohse, *Electrochemical Impedance Spectroscopy in Electroanalytical Methods*, Springer, Berlin, **2002**.
[3] A. Lasia, in *Modern Aspects of Electrochemistry* (Eds.: B. E. Conway, J. O. Bockris, R. E. White), Kluwer Academic, New York, **1999**, pp. 143–248.
[4] A. Lasia, *Electrochemical Impedance Spectroscopy and Its Applications*, **2014**.
[5] V. F. Lvovich, *Impedance Spectroscopy*, John Wiley & Sons, Inc., Hoboken, NJ, **2012**.
[6] D. D. Macdonald, *Electrochim. Acta* **2006**, *51*, 1376–1388.
[7] A. J. Bard, G. Inzelt, F. Scholz, *Electrochemical Dictionary*, Springer, Berlin-Heidelberg, **2012**.
[8] S. Anantharaj, S. Noda, *ChemElectroChem* **2020**, *7*, 2297–2308.
[9] T. Osaka, K. Naoi, *Bull. Chem. Soc. Jpn.* **1982**, *55*, 36–40.
[10] J. S. Yoo, S.-M. Park, *Anal. Chem.* **2000**, *72*, 2035–2041.
[11] T. Osaka, H. Nara, D. Mukoyama, T. Yokoshima, *J. Electrochem. Sci. Technol.* **2013**, *4*, 157–162.
[12] T. Osaka, D. Mukoyama, H. Nara, *J. Electrochem. Soc.* **2015**, *162*, A2529–A2537.
[13] T. Yokoshima, D. Mukoyama, K. Nakazawa, Y. Gima, H. Isawa, H. Nara, T. Momma, T. Osaka, *Electrochim. Acta* **2015**, *180*, 922–928.
[14] T. Yokoshima, D. Mukoyama, H. Nara, S. Maeda, K. Nakazawa, T. Momma, T. Osaka, *Electrochim. Acta* **2017**, *246*, 800–811.
[15] D. D. Macdonald, in *Corrosion Science ECS Proceedings*, The Electrochemical Society, Inc., Pennington, NJ, **2002**, pp. 72–88.
[16] S. Goldman, *Transformation Calculus and Electrical Transients*, Prentice-Hall, Englewood Cliffs, NJ, **1950**.
[17] J. R. Macdonald, *Impedance Spectroscopy*, John Wiley, New York, **1987**.
[18] D. D. Macdonald, M. C. H. McKubre, in *Electrochemical Corrosion Testing* (Eds.: F. Mansfield, U. Bertocci), ASTM International, West Conshohocken, PA, **1981**, pp. 110–149.
[19] E. Barsoukov, J. R. Macdonald, *Impendance Spectroscopy*, John Wiley & Sons, Inc., Hoboken, NJ, **2018**.
[20] E. Katz, I. Willner, *Electroanalysis* **2003**, *15*, 913–947.
[21] F.-G. Banica, *Chemical Sensors and Biosensors: Fundamentals and Applications*, John Wiley & Sons, Inc., Chichester, United Kingdom, **2012**.
[22] J. Janata, *Principles of Chemical Sensors*, Dordrecht, **2009**.

[23] J. G. Webster, H. Eren, Eds., *Measurement, Instrumentation, and Sensors Handbook*, CRC Press, Boca Raton, FL, **2014**.
[24] S. Bhattacharya, A. K. Agarwal, N. Chanda, A. Pandey, A. K. Sen, Eds., *Environmental, Chemical and Medical Sensors*, Springer Nature, Singapore, **2018**.
[25] U. Pliquett, *Food Engineering Reviews* **2010**, *2*, 74–94.
[26] D. El Khaled, N. N. Castellano, J. A. Gazquez, R. M. G. Salvador, F. Manzano-Agugliaro, *J. Cleaner Prod.* **2017**, *140*, 1749–1762.
[27] M. Tabinor, E. Elphick, D. Michael, C. S. Kwok, M. Lambie, S. J. Davies, *Sci. Rep.* **2018**, *8*, 1–14.
[28] S. Grimnes, Ø. G. Martinsen, *Bioimpedance and Bioelectricity Basics*, Elsevier, London, **2015**.
[29] M. D. Van Loan, L. E. Kopp, J. C. King, W. W. Wong, P. L. Mayclin, *J. Appl. Physiol.* **1995**, *78*, 1037–1042.
[30] M. Y. Jaffrin, H. Morel, *Med. Eng. Phys.* **2008**, *30*, 1257–1269.
[31] Z. Moore, D. Patton, S. L. Rhodes, T. O'Connor, *Int. Wound J.* **2016**, 331–337.
[32] G. G. Láng, *Electrochemistry* **2020**, *1*, 104–123.
[33] M. P. Bolton, L. C. Ward, A. Khan, I. Campbell, P. Nightingale, O. Dewit, M. Elia, *Physiological Measurement* **1998**, *19*, 235–245.
[34] P. E. Wellstead, *Frequency Response Analysis*, Farnborough, **1997**.
[35] Z. Stoynov, in *Materials for Lithium-Ion Batteries, NATO Science Series, 3. High Technology, 85* (Eds.: C. Julien, Z. Stoynov), Kluwer Academic Publishers, Sozopol, Bulgaria, **2000**, p. 359.
[36] D. Vladikova, *Bulg. Chem. Commun.* **2018**, *50*, 7–20.
[37] H. W. Bode, *Network Analysis and Feedback Amplifier Design*, D. Van Nostrand Co., Inc., New York, **1957**.
[38] L. D. Landau, E. M. Lifshitz, in *Course of Theoretical Physics, Vol.8*, Pergamon Press, Oxford, **1960**.
[39] E. C. Titchmarsh, *Introduction to the Theory of Fourier Integrals*, Oxford University Press, Oxford, **1948**.
[40] A. Papoulis, *The Fourier Integral and Its Applications*, McGraw-Hill, New York, **1962**.
[41] M. M. Jaksic, J. Newman, *J. Electrochem. Soc.* **1986**, *133*, 1097–1101.
[42] D. D. Macdonald, M. Urquidi-Macdonald, *J. Electrochem. Soc.* **1985**, *132*, 2316–2319.
[43] M. Urquidi-Macdonald, S. Real, D. D. Macdonald, *J. Electrochem. Soc.* **2018**, *133*, 2018–2024.
[44] D. D. Macdonald, M. Urquidi-Macdonald, *J. Electrochem. Soc.* **1990**, *137*, 515–517.
[45] H. Song, D. D. Macdonald, *J. Electrochem. Soc.* **1991**, *138*, 1408–1410.
[46] B. A. Boukamp, *J. Electrochem. Soc.* **1995**, *142*, 1885–1894.
[47] M. K. Brachman, J. Ross Macdonald, *Physica* **1954**, *20*, 1266–1270.
[48] F. Ciucci, *J. Electrochem. Soc.* **2020**, *167*, 126503.
[49] J. Liu, T. H. Wan, F. Ciucci, *Electrochim. Acta* **2020**, *357*, 136864.
[50] M. Schönleber, D. Klotz, E. Ivers-Tiffée, *Electrochim. Acta* **2014**, *131*, 20–27.
[51] J. Dambrowski, in *IECON 2013 – the 39th Annual Conference of the IEEE Industrial Electronics Society*, Vienna, Austria, **2013**.
[52] R. L. Van Meirhaeghe, E. C. Dutoit, F. Cardon, W. P. Gomes, *Electrochim. Acta* **1976**, *21*, 39–43.
[53] C. Gabrielli, M. Keddam, H. Takenouti, in *Electrochemical Impedance: Analysis and Interpretation* (Eds.: J. Scully, D. Silverman, M. Kendig), ASTM International, West Conshohocken, PA, **1993**, pp. 140–153.
[54] M. E. Orazem, B. Tribollet, *Electrochemical Impedance Spectroscopy*, ECS-The Electrochemical Society, Pennington, NJ, **2008**.
[55] G. G. Láng, L. Kocsis, G. Inzelt, *Electrochim. Acta* **1993**, *38*, 1047–1049.
[56] G. Inzelt, G. G. Láng, in *Electropolymerization: Concepts, Materials and Applications* (Eds.: S. Cosnier, A. Karyakin), Wiley-VCH, Weinheim, **2010**, pp. 51–76.
[57] F. W. King, *Hilbert Transforms*, Cambridge, Cambridge, UK, **2009**.
[58] M. Urquidi-Macdonald, S. Real, D. D. Macdonald, *Electrochim. Acta* **1990**, *35*, 1559–1566.
[59] B. Hirschorn, M. E. Orazem, *J. Electrochem. Soc.* **2009**, *156*, C345–C351.
[60] B. A. Boukamp, *Solid State Ionics* **1993**, *62*, 131–141.
[61] A. Sadkowski, *J. Electroanal. Chem.* **2004**, *573*, 241–253.
[62] C. You, M. A. Zabara, M. E. Orazem, B. Ulgut, *J. Electrochem. Soc.* **2020**, *167*, 020515.
[63] A. E. Bolzán, *Electrochim. Acta* **2013**, *113*, 706–718.
[64] K. Martinusz, G. Láng, G. Inzelt, *J. Electroanal. Chem.* **1997**, *433*, 1–8.
[65] G. Inzelt, G. Láng, *J. Electroanal. Chem.* **1994**, *378*, 39–49.
[66] P. Agarwal, M. E. Orazem, L. H. Garcia-Rubio, *J. Electrochem. Soc.* **1995**, *142*, 4159–4168.
[67] M. E. Orazem, J. M. Esteban, O. C. Moghissi, *Corrosion* **1991**, *47*, 248–259.
[68] C. A. Schiller, F. Richter, E. Gülzow, N. Wagner, *Phys. Chem. Chem. Phys.* **2001**, *3*, 374–378.
[69] B. A. Boukamp, J. Ross Macdonald, *Solid State Ionics* **1994**, *74*, 85–101.
[70] T. J. VanderNoot, *J. Electroanal. Chem.* **1992**, *322*, 9–24.
[71] Metrohm, "NOVA 2.1.2 User Manual," can be found under https://www.ecochemie.nl/download/NovaSoftware/NOVA_2.1.2_User_Manual.pdf, **2017**.
[72] F. J. Harris, *Proc. IEEE* **1978**, *66*, 51–83.
[73] R. W. Hamming, *Digital Filters*, Prentice Hall, Englewood Cliffs, NJ, **1978**.
[74] S. Butterworth, *Experimental Wireless and the Wireless Engineer* **1930**, *7*, 536–541.
[75] A. N. Akansu, R. A. Haddad, *Multiresolution Signal Decomposition: Transforms, Subbands, and Wavelets.*, Academic Press, Boston, MA, **1992**.
[76] K. Darowicki, A. Zieliński, *Fluctuation and Noise Letters* **2006**, *6*, L215–L225.
[77] Z. Stoynov, *Bulg. Chem. Commun.* **2018**, *50*, 123–130.
[78] D. Gabor, *The Institution of Electrical Engineers* **1946**, *93*, 429–441.
[79] D. Gabor, *The Institution of Electrical Engineers* **1946**, *93*, 442–445.
[80] E. Sejdić, I. Djurović, J. Jiang, *Digital Signal Processing* **2009**, *19*, 153–183.
[81] K. Darowicki, A. Zieliński, *J. Electroanal. Chem.* **2001**, *504*, 201–207.
[82] K. Darowicki, *J. Electroanal. Chem.* **2000**, *486*, 101–105.
[83] K. Darowicki, J. Orlikowski, G. Lentka, *J. Electroanal. Chem.* **2000**, *486*, 106–110.
[84] K. Darowicki, P. Ślepski, *Electrochem. Commun.* **2004**, *6*, 898–902.
[85] K. Darowicki, P. Ślepski, M. Szociński, *Prog. Org. Coat.* **2005**, *52*, 306–310.
[86] G. Blanc, C. Gabrielli, M. Keddam, *Electrochim. Acta* **1975**, *20*, 687–689.
[87] S. C. Creason, J. W. Hayes, D. E. Smith, *J. Electroanal. Chem.* **1973**, *47*, 9–46.
[88] J. E. Garland, C. M. Pettit, D. Roy, *Electrochim. Acta* **2004**, *49*, 2623–2635.
[89] E. Van Gheem, R. Pintelon, J. Vereecken, J. Schoukens, A. Hubin, P. Verboven, O. Blajiev, *Electrochim. Acta* **2004**, *49*, 4753–4762.
[90] E. Van Gheem, R. Pintelon, A. Hubin, J. Schoukens, P. Verboven, O. Blajiev, J. Vereecken, *Electrochim. Acta* **2006**, *51*, 1443–1452.
[91] O. L. Blajiev, R. Pintelon, A. Hubin, *J. Electroanal. Chem.* **2005**, *576*, 65–72.
[92] Y. Van Ingelgem, E. Tourwé, O. Blajiev, R. Pintelon, A. Hubin, *Electroanalysis* **2009**, *21*, 730–739.
[93] T. Breugelmans, E. Tourwé, J. B. Jorcin, A. Alvarez-Pampliega, B. Geboes, H. Terryn, A. Hubin, *Prog. Org. Coat.* **2010**, *69*, 215–218.
[94] T. Breugelmans, J. Lataire, T. Muselle, E. Tourwé, R. Pintelon, A. Hubin, *Electrochim. Acta* **2012**, *76*, 375–382.
[95] A. Battistel, G. Du, F. La Mantia, *Electroanalysis* **2016**, *28*, 2346–2353.
[96] A. Battistel, F. La Mantia, *Electrochim. Acta* **2019**, *304*, 513–520.
[97] E. Madej, S. Klink, W. Schuhmann, E. Ventosa, F. La Mantia, *J. Power Sources* **2015**, *297*, 140–148.
[98] G. A. Ragoisha, A. S. Bondarenko, N. P. Osipovich, E. A. Streltsov, *J. Electroanal. Chem.* **2004**, *565*, 227–234.
[99] R. L. Sacci, D. A. Harrington, *ECS Trans.* **2009**, *19*, 31–42.
[100] R. L. Sacci, D. A. Harrington, *ECS Trans.* **2009**, *19*, 123–129.
[101] R. L. Sacci, F. Seland, D. A. Harrington, *Electrochim. Acta* **2014**, *131*, 13–19.
[102] B. Savova-Stoynov, Z. B. Stoynov, *Mech. Corros. Prop. A* **1991**, *59–60*, 273–282.
[103] Z. Stoynov, *Electrochim. Acta* **1993**, *38*, 1919–1922.
[104] G. S. Popkirov, *Electrochim. Acta* **1996**, *41*, 1023–1027.
[105] Z. B. Stoynov, B. S. Savova-Stoynov, *J. Electroanal. Chem.* **1985**, *183*, 133–144.
[106] B. Savova-Stoynov, Z. B. Stoynov, *Electrochim. Acta* **1992**, *37*, 2353–2355.
[107] N. Wagner, E. Gülzow, *J. Power Sources* **2004**, *127*, 341–347.
[108] W. Meißner, Eine neue Methode der Messung und Auswertung von Impedanzspektren an Elektroden, angewandt auf die Kinetik der anodischen Oxydation von Silber in alkalischer Lösung, Thesis, University of Erlangen-Nürnberg, **1974**.
[109] H. Göhr, F. Richter, *Zeitschrift für Phys. Chemie* **1979**, *115*, 69–88.
[110] M. Ujvári, D. Zalka, S. Vesztergom, S. Eliseeva, V. Kondratiev, G. G. Láng, *Bulg. Chem. Commun.* **2017**, *49*, 106–113.
[111] D. Zalka, N. Kovács, K. Szekeres, M. Ujvári, S. Vesztergom, S. Eliseeva, V. Kondratiev, G. G. Láng, *Electrochim. Acta* **2017**, *247*, 321–332.

[112] D. Zalka, S. Vesztergom, M. Ujvári, G. G. Láng, *J. Electrochem. Sci. Eng.* **2018**, *8*, 151–162.
[113] V. Horvat-Radošević, K. Kvastek, K. M. Košiček, *Bulg. Chem. Commun.* **2017**, *49*, 119–127.
[114] K. M. Košiček, V. Horvat-Radošević, K. Kvastek, *Croat. Chem. Acta* **2018**, *91*, 463–473.
[115] S. V. G. G. Láng, K. J. Szekeres, M. Ujvári, in *The 71st Annual Meeting of the International Society of Electrochemistry*, Belgrade, Serbia, **2020**.
[116] Installer package of the "Software for the correction of 'impedance' data measured under non-stationary conditions" can be found at http://electro.chem.elte.hu:5080/members/vesztergom/index_en.htm, **2021**.
[117] R. J. Beerends, H. G. ter Morsche, J. C. van den Berg, E. M. van de Vrie-Fourier, *Fourier and Laplace Transforms*, Cambridge University Press, Cambridge, **2003**.
[118] P. Dyke, *An Introduction to Laplace Transforms and Fourier Series*, Springer, London, **2001**.
[119] R. P. Kanwal, *Linear Integral Equations – Theory and Technique*, Academic Press, New York, **1971**.
[120] M. Legua, L. M. Sánchez-Ruiz, *Entropy* **2017**, *19*, 215.
[121] R. Dautray, J.-L. Lions, *Mathematical Analysis and Numerical Methods for Science and Technology, Volume 4, Integral Equations and Numerical Methods*, Springer, Berlin, **1990**.

Manuscript received: January 21, 2021
Revised manuscript received: February 27, 2021
Accepted manuscript online: March 1, 2021